

Characterization of Manganese(II) Binding Site Mutants of Manganese Peroxidase[†]Katsuyuki Kishi, Margo Kusters-van Someren,[‡] Mary B. Mayfield, Jie Sun, Thomas M. Loehr, and Michael H. Gold*

Department of Chemistry, Biochemistry, and Molecular Biology, Oregon Graduate Institute of Science & Technology, Portland, Oregon 97291-1000

Received March 19, 1996; Revised Manuscript Received May 1, 1996[®]

ABSTRACT: A series of site-directed mutants, E35Q, E39Q, and E35Q-D179N, in the gene encoding manganese peroxidase isozyme 1 (*mnp1*) from *Phanerochaete chrysosporium*, was created by overlap extension, using the polymerase chain reaction. The mutant genes were expressed in *P. chrysosporium* during primary metabolic growth under the control of the glyceraldehyde-3-phosphate dehydrogenase promoter. The mutant manganese peroxidases (MnPs) were purified and characterized. The molecular masses of the mutant proteins, as well as UV–vis spectral features of their oxidized states, were very similar to those of the wild-type enzyme. Resonance Raman spectral results indicated that the heme environment of the mutant MnP proteins also was similar to that of the wild-type protein. Steady-state kinetic analyses of the E35Q and E39Q mutant MnPs yielded K_m values for the substrate Mn^{II} that were ~50-fold greater than the corresponding K_m value for the wild-type enzyme. Likewise, the k_{cat} values for Mn^{II} oxidation were ~300-fold lower than that for wild-type MnP. With the E35Q-D179N double mutant, the K_m value for Mn^{II} was ~120-fold greater, and the k_{cat} value was ~1000-fold less than that for the wild-type MnP1. Transient-state kinetic analysis of the reduction of MnP compound II by Mn^{II} allowed the determination of the equilibrium dissociation constants (K_D) and first-order rate constants for the mutant proteins. The K_D values were approximately 100-fold higher for the single mutants and approximately 200-fold higher for the double mutant, as compared with the wild-type enzyme. The first-order rate constants for the single and double mutants were ~200-fold and ~4000-fold less, respectively, than that of the wild-type enzyme. In contrast, the K_m values for H_2O_2 and the rates of compound I formation were similar for the mutant and wild-type MnPs. The second-order rate constants for *p*-cresol and ferrocyanide reduction of the mutant compounds II also were similar to those of the wild-type enzyme.

White-rot basidiomycete fungi are capable of degrading the plant cell wall polymer lignin (Gold et al., 1989; Kirk & Farrell, 1987; Buswell & Odier, 1987) and a variety of aromatic pollutants (Bumpus & Aust, 1987; Hammel, 1989; Valli & Gold, 1991; Valli et al., 1992). When cultured under ligninolytic conditions, the white-rot fungus *Phanerochaete chrysosporium* secretes two families of extracellular peroxidases, lignin peroxidase (LiP)¹ and manganese peroxidase (MnP), which, along with an H_2O_2 -generating system, comprise the major extracellular components of its lignin-degrading system (Kirk & Farrell, 1987; Buswell & Odier, 1987; Gold & Alic, 1993; Wariishi et al., 1991; Bao et al., 1994; Hammel et al., 1993). Both LiP and MnP are able to depolymerize lignin *in vitro* (Wariishi et al., 1991; Bao et

al., 1994; Hammel et al., 1993). Moreover, MnP activity is found in all white-rot fungi known to degrade lignin (Hatakka, 1994; Perie & Gold, 1991; Orth et al., 1993).

P. chrysosporium MnP has been purified and characterized extensively by a variety of biochemical and biophysical methods (Gold et al., 1989; Gold & Alic, 1993; Glenn & Gold, 1985; Glenn et al., 1986; Wariishi et al., 1992). In addition, the sequences of cDNA and genomic clones encoding several *P. chrysosporium* MnP isozymes (*mnp1* and *mnp2*) have been determined (Gold & Alic, 1993; Pribnow et al., 1989; Pease et al., 1989; Godfrey et al., 1990; Mayfield et al., 1994a). Spectroscopic studies and DNA sequences suggest that the heme environment of MnP is similar to that of other plant and fungal peroxidases (Glenn et al., 1986; Wariishi et al., 1988, 1992; Pribnow et al., 1989; Harris et al., 1991; Banci et al., 1992; Dunford & Stillman, 1976; Mino et al., 1988). Kinetic and spectral characterization of the oxidized intermediates, MnP compounds I, II, and III, indicates that the catalytic cycle of MnP is similar to that of horseradish peroxidase and LiP (Gold et al., 1989; Glenn et al., 1986; Wariishi et al., 1988, 1992; Renganathan & Gold, 1986). The crystal structures of both LiP and MnP have been reported (Edwards et al., 1993; Poulos et al., 1993; Piontek et al., 1993; Sundaramoorthy et al., 1994). These structures confirm that the heme environments of MnP and LiP are similar to those of cytochrome *c* peroxidase and plant and fungal peroxidases (Poulos et al., 1993; Sundaramoorthy et al., 1994). However, the crystal structure of MnP revealed

[†] Supported by grants from the National Science Foundation (MCB-9405978 to M.H.G.), the U.S. Department of Energy, Office of Basic Energy Sciences (DE-FG06-92ER20093 to M.H.G.), and the National Institutes of Health (GM34468 to T.M.L.), and by a National Science Foundation Instrumentation grant (BIR9216592 to T.M.L. and M.H.G.).

* To whom correspondence should be addressed at the Department of Chemistry, Biochemistry, and Molecular Biology, Oregon Graduate Institute of Science & Technology, P.O. Box 91000, Portland, OR 97291-1000. Telephone: 503-690-1076. Fax: 503-690-1464.

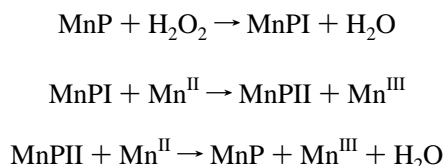
[‡] Present address: Section of Molecular Genetics of Industrial Microorganisms, Wageningen Agricultural University, Dreijenlaan 2, 6703 HA Wageningen, The Netherlands.

[®] Abstract published in *Advance ACS Abstracts*, June 15, 1996.

¹ Abbreviations: LiP, lignin peroxidase; MnP, manganese peroxidase; MnP1, manganese peroxidase isozyme 1; *mnp1*, gene encoding MnP1; PAGE, polyacrylamide gel electrophoresis; PCR, polymerase chain reaction; rMnP1, recombinant wild-type manganese peroxidase isozyme 1; SDS, sodium dodecyl sulfate.

a cation binding site. The ligands to this proposed Mn^{II} binding site are Glu35, Glu39, Asp179, a heme propionate, and two H_2O molecules (Sundaramoorthy et al., 1994). MnP is unique in its ability to oxidize Mn^{II} to Mn^{III} (Glenn & Gold, 1985; Glenn et al., 1986; Wariishi et al., 1992) as shown in Scheme 1.

Scheme 1



The enzyme-generated Mn^{III} is stabilized by organic acid chelators such as oxalate which is also secreted by the fungus (Wariishi et al., 1992; Kishi et al., 1994; Kuan et al., 1993). The Mn^{III} –organic acid complex oxidizes phenolic substrates, including lignin substructure model compounds (Tuor et al., 1992) and aromatic pollutants (Valli & Gold, 1991; Valli et al., 1992; Joshi & Gold, 1993), as well as possible mediator molecules (Bao et al., 1994; Wariishi et al., 1989b).

We recently developed a homologous expression system for MnP isozyme 1 (MnP1) (Mayfield et al., 1994b). In this system, the *P. chrysosporium* glyceraldehyde-3-phosphate dehydrogenase (*gpd*) promoter is used to drive expression of the *mnp1* gene during the primary metabolic growth phase when endogenous MnP is not expressed. This expression system produces recombinant MnP1 (rMnP1) in amounts comparable to the endogenous MnPs produced by the wild-type strain (Mayfield et al., 1994b). Previously, we used this expression system and the polymerase chain reaction (PCR) to create a site-directed mutation in which Asp179, one of the potential Mn^{II} binding ligands in MnP, was converted to an Asn (Kusters-van Someren et al., 1995). Kinetic and spectroscopic analyses demonstrated that this mutation significantly affected the oxidation of Mn^{II} , probably by decreasing the affinity of the enzyme for Mn^{II} , confirming that Asp179 is a Mn^{II} ligand. To further characterize the Mn^{II} binding site, we have mutated the putative Mn^{II} ligands Glu35 and Glu39 and characterized these single mutants and an E35Q-D179N double mutant spectroscopically and kinetically.

MATERIALS AND METHODS

Organisms. *P. chrysosporium* wild-type strain OGC101, auxotrophic strain OGC107-1 (Ade1), and prototrophic transformants were maintained as described (Mayfield et al., 1994b; Alic et al., 1990). *Escherichia coli* XL1-Blue and DH5 α F' were used for subcloning plasmids.

Oligodeoxyribonucleotides. Four oligonucleotides were each used for site-directed mutagenesis of Glu35 and Glu39 of *mnp1* (Pribnow et al., 1989; Godfrey et al., 1990). Oligonucleotide N10_{norm} is a 17-mer corresponding to *mnp1* positions 14–30. Oligonucleotide B9_{rev} is complementary to the *mnp1* sequence over nucleotide positions 592–608. Oligonucleotides Q35_{norm} and Q35_{rev} are a 27-mer and a 29-mer, respectively, and are partially overlapping: Q35_{norm} spans nucleotides 219–245, and Q35_{rev} is complementary to nucleotides 207–235. Oligonucleotides Q39_{norm} and Q39_{rev} are 28-mers and are again partially overlapping:

Q39_{norm} spans nucleotides 289–316, and Q39_{rev} is complementary to nucleotides 278–305. Oligonucleotides were synthesized at the Center for Gene Research and Biotechnology, Oregon State University, Corvallis, OR. Q35_{norm} and Q35_{rev} contain the preferred codon and anticodon (Ritch & Gold, 1992), respectively, for Gln, CAG replacing GAA, which encodes Glu35. Q39_{norm} and Q39_{rev} also contain the preferred codon and anticodon, respectively, for Gln, CAG replacing GAG, which encodes Glu39.

Site-Directed Mutagenesis by PCR. A 544-bp *NotI*–*Bpu1102I* fragment containing the E35Q or E39Q mutation was generated by overlap extension (Kusters-van Someren et al., 1995; Ho et al., 1989) using the polymerase chain reaction (PCR). Two fragments which partially overlap were generated by using either oligonucleotides N10_{norm} and Q35_{rev} (or Q39_{rev}) or oligonucleotides Q35_{norm} (or Q39_{norm}) and B9_{rev} under the conditions described (Kusters-van Someren et al., 1995). The products of both reactions were analyzed by electrophoresis on a 1% agarose gel, and the desired fragments were excised and purified using GeneClean (Bio101). The partially overlapping fragments were combined and used as template DNA in a third reaction with oligonucleotides N10_{norm} and B9_{rev} to generate a 593-bp PCR fragment under the same conditions (Kusters-van Someren et al., 1995). The final PCR product was analyzed by agarose gel electrophoresis, excised, purified by GeneClean, and digested with *NotI* and *Bpu1102I* (New England Biolabs).

Construction of pAGM6, -8, and -9. The *NotI*–*Bpu1102I* fragments containing the E35Q and E39Q mutations were first subcloned into pGM1 (Kusters-van Someren et al., 1995), containing unique *NotI*–*Bpu1102I* sites, replacing the wild-type *mnp1* fragment with the mutant fragment, to generate pGM8 and pGM9, respectively. For the E35Q-D179N double mutation, the *NotI*–*Bpu1102I* fragment containing the E35Q mutation was subcloned into pGM4, which contains the D179N mutation (Kusters-van Someren et al., 1995), to generate pGM6. The entire *NotI*–*Bpu1102I* fragments were analyzed by double-stranded DNA sequencing as described (Kusters-van Someren et al., 1995). Subsequently, the 4.0-kb *XbaI*–*EcoRI* fragments of pGM6, -8, and -9, containing the *gpd* promoter and the mutated *mnp1* genes, were subcloned into pOGI18 (Godfrey et al., 1994), generating pAGM6, -8, and -9, respectively. The presence of the mutations in pAGM6, -8, and -9 was confirmed by double-stranded DNA sequencing of the appropriate sequences, using oligonucleotide N10_{norm} as a primer.

Transformation of *Phanerochaete chrysosporium*. *P. chrysosporium* strain Ade1 (Gold et al., 1982) was transformed as described previously (Mayfield et al., 1994a,b; Alic et al., 1990), using 1 μg of pAGM6, -8, or -9 as transforming DNA. Transformants were transferred to minimal slants (Mayfield et al., 1994a,b; Alic et al., 1990) to confirm adenine prototrophy and assayed for MnP activity using the *o*-anisidine plate assay as described (Mayfield et al., 1994b). Transformants with the strongest activity were purified by fruiting as described (Alic et al., 1987), and the progeny were rescreened for MnP activity by the *o*-anisidine plate assay.

Production and Purification of the MnP Mutant Proteins. Cultures were maintained on slants and grown in liquid cultures from conidial inocula (Mayfield et al., 1994b; Kusters-van Someren et al., 1995). The MnP mutant proteins

were purified from the extracellular medium as described for the wild-type recombinant MnP1 (Mayfield et al., 1994b), except that hydrophobic interaction column chromatography was employed as the initial step. Ammonium sulfate (1.0 M) was added to the concentrated extracellular medium after which the mixture was applied to a phenyl-sepharose CL-6B column (2.5 × 15 cm), equilibrated with 20 mM sodium acetate (pH 4.5), containing 1.0 M ammonium sulfate. The column was eluted at 4 °C with a linear ammonium sulfate gradient (1.0–0.2 M). The fractions containing MnP activity were concentrated and desalted by membrane ultrafiltration. MnP mutant proteins were purified further by a combination of Cibacron Blue 3GA agarose column chromatography and fast-protein liquid chromatography using a Mono Q column (Pharmacia), as described (Mayfield et al., 1994b; Kusters-van Someren et al., 1995).

SDS-PAGE and Western Blot Analysis. Sodium dodecyl sulfate–polyacrylamide gel electrophoresis (SDS-PAGE) was performed using a 12% Tris–glycine gel system (Laemmli, 1970) and a Mini-Protein II apparatus (Bio-Rad). The gels were stained with Coomassie blue. For Western (immunoblot) analysis, proteins were electroblotted (Sambrook et al., 1989) onto nitrocellulose (Micron Separations, Inc.), and MnP proteins were detected as described (Mayfield et al., 1994b).

Enzyme Assays and Spectroscopic Procedures. Mn^{II} oxidation by MnP was measured by following the formation of Mn^{III}–malonate at 270 nm as previously described (Wariishi et al., 1992). The oxidation of ferrocyanide by MnP was followed at 420 nm using the absorptivity of ferricyanide, 1 mM⁻¹ cm⁻¹ (Cheddar et al., 1989). UV absorption spectra of the various oxidation states of MnP mutant proteins were recorded at room temperature using a Shimadzu UV-260 spectrophotometer. The enzyme was maintained in 20 mM potassium malonate, pH 4.5. The ionic strength of the buffers was adjusted to 0.1 M using K₂SO₄. Enzyme concentrations were determined at 406 nm, the Soret absorbance maximum of the native enzyme, using an absorptivity of 129 mM⁻¹ cm⁻¹ (Glenn & Gold, 1985). Compound I of the MnP mutants was prepared by mixing 1.0 equiv of H₂O₂ with native enzyme. Compound II was prepared by the successive addition of 1.0 equiv of H₂O₂ and 1.0 equiv of ferrocyanide to the native enzyme.

Kinetic Analysis. To determine apparent K_m and k_{cat} values for Mn^{II} and ferrocyanide, 1/initial velocity versus 1/[substrate] were plotted at fixed concentrations of H₂O₂ (0.1 mM). Reaction mixtures contained mutant MnP protein (10 µg/mL), H₂O₂, and MnSO₄ (0.5–5.0 mM) or ferrocyanide (1.0–5.0 mM) in 50 mM sodium malonate, pH 4.5. To determine apparent K_m values for H₂O₂, 1/initial velocity versus 1/[H₂O₂] were plotted at 5 mM Mn^{II}. Transient state kinetic experiments on the formation of compound I and the reduction of compound II were carried out at 25.0 ± 1.0 °C using a Dionex DC37 stopped-flow photometer (dead time 2.7 ms) equipped with a 75-W xenon lamp and interfaced with a Nicolet Explorer III scope kindly provided by Prof. M. Schimerlik, Oregon State University. One reservoir contained buffer and the enzyme (2 µM for compound I formation and 4 µM for compound II reduction experiments). The other reservoir contained the substrate (H₂O₂, Mn^{II}, *p*-cresol, or ferrocyanide) in water in at least 10-fold excess with respect to the enzyme. The formation of MnP compound I in 20 mM potassium succinate, pH 4.5 (ionic

strength 0.1 M, adjusted with K₂SO₄), was followed at 397 nm, the isosbestic point between compounds I and II. The reduction of MnP compound II in 20 mM potassium malonate, pH 4.5, or 1 mM potassium oxalate, pH 4.6 (ionic strength 0.1 M, adjusted with K₂SO₄), was followed at 406 nm. Compound II of MnP mutant proteins was freshly prepared for each experiment, and the reaction was initiated by adding the reducing substrate in 10-fold excess. All of the kinetic traces displayed single-exponential character from which pseudo-first-order rate constants were calculated. Several substrate concentrations were used, and plots of pseudo-first-order rate constants versus substrate concentration were obtained.

Resonance Raman Spectroscopy. Resonance Raman (rR) spectra were obtained on a custom spectrograph consisting of a McPherson (Acton, MA) Model 2061/207 monochromator operated at a focal length of 0.67 m and a Princeton Instruments (Trenton, NJ) LN1100 CCD detector with a Model ST-130 controller. Laser excitation was from Coherent (Santa Clara, CA) Innova 302 krypton (413.1 nm) and Innova 90-6 argon (514.5 nm) lasers. The laser lines were filtered through Applied Photophysics (Leatherhead, U.K.) prism monochromators to remove plasma emissions. Incident laser power at the sample was ~20 mW (413.1 nm) and ~55 mW (514.5 nm). Spectra were collected in a 90°-scattering geometry from solution samples contained in glass capillary tubes at room temperature. Rayleigh scattering was attenuated by use of Kaiser Optical (Ann Arbor, MI) notch or super-notch filters. Spectral resolution was set to ~3.0 cm⁻¹. Indene and CCl₄ served as frequency and polarization standards, respectively. Data were calibrated and analyzed with GRAMS/386 spectroscopic software (Galactic Industries Corp., Salem NH). The concentrations of MnP protein for rR studies were 100–200 µM in phosphate buffer (20 mM, pH 6.0) at a constant ionic strength of 0.1 (adjusted with Na₂SO₄).

Chemicals. Phenyl-Sepharose CL-6B, Cibacron Blue 3GA agarose, potassium ferrocyanide, and H₂O₂ (30% solution) were obtained from Sigma. The concentration of the H₂O₂ stock solution was determined as described (Cotton & Dunford, 1973). *p*-Cresol was obtained from Aldrich and was purified by silica gel thin-layer chromatography (solvent hexane/ethyl acetate, 3:1) before use. All other chemicals were reagent grade. Solutions were prepared using deionized water obtained from a Milli Q purification system (Millipore).

RESULTS

Expression and Purification of Mutant Proteins. The presence of the E35Q and E39Q single mutations and the E35Q-D179N double mutation was confirmed by double-stranded DNA sequencing of the altered cassettes in both pGM6, -8, and -9 and the complete transformation vectors pAGM6, -8, and -9, respectively. Transformants which exhibited readily detectable MnP activity on plate assays were selected and purified by fruiting as described (Alic et al., 1990). The purified transformants expressed extracellular recombinant MnP protein within 3 days after inoculation of liquid high-carbon, high-nitrogen agitated cultures, as verified by Western (immunoblot) detection (data not shown). Endogenous MnP is not expressed under these conditions. The amounts of mutant protein secreted by the pAGM6, -8,

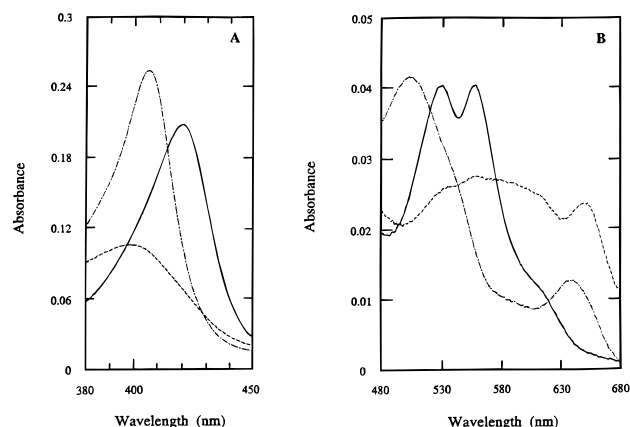


FIGURE 1: Electronic absorption spectra of oxidized states of the MnP E35Q-D179N double mutant. Comparison of UV/vis absorption spectra of native MnP E35Q-D179N (— · —), compound I (— · —), and compound II (—). Spectra were recorded in 20 mM potassium malonate, pH 4.5, at 25 °C. The enzyme concentrations were 2 μ M (A, Soret spectra) and 4 μ M (B, visible spectra). MnP E35Q-D179N compound I (— · —) was prepared by adding 1 equiv of H_2O_2 to the native enzyme in 20 mM potassium malonate, pH 4.5 ($\mu = 0.1$). MnP E35Q-D179N compound II (—) was prepared by the successive additions of 1.0 equiv of H_2O_2 and 1.0 equiv of ferrocyanide to the native enzyme in the same buffer.

and -9 transformants were comparable to the levels of recombinant wild-type MnP1 (rMnP1) we reported previously (Mayfield et al., 1994b), as estimated by Western immunoblot analysis (data not shown). However, the transformants exhibited low Mn^{II} -oxidizing activity, as measured by the formation of the Mn^{III} -malonate complex (Wariishi et al., 1992). MnP proteins E35Q, E39Q, and E35Q-D179N were purified using phenyl-sepharose, Blue Agarose, and Mono Q chromatographies (Mayfield et al., 1994a,b; Kusters-van Someren et al., 1995). Phenyl-Sepharose replaced DEAE-Sepharose (Mayfield et al., 1994b; Kusters-van Someren et al., 1995) as an initial purification step since the yield of MnP protein was higher. The major peak eluted from the Mono Q column in the same fraction as rMnP1, when the latter was chromatographed under identical conditions (data not shown) (Mayfield et al., 1994b). Furthermore, the molecular masses (46 kDa) of the MnP mutant proteins were identical to those of rMnP1 and wild-type MnP1 (data not shown).

Spectral Properties of MnP Mutant Proteins. Figure 1 shows the absorption spectra of the native, compound I, and compound II states of the MnP E35Q-D179N double mutant protein. The native protein exhibited a Soret band at 406 nm and visible bands at 500 and 640 nm. The Soret band of compound I was decreased with respect to native MnP and blue-shifted from 406 to 397 nm. The visible region of compound I displayed a peak at 650 nm with a broad absorption from 530 to 600 nm. The addition of 1.0 equiv of ferrocyanide to compound I yielded a spectrum for compound II with maxima at 420, 528, and 555 nm. Similar absorption spectra of the native, compound I, and compound II states were observed for the MnP E35Q and E39Q single mutant proteins (data not shown). All of the spectral maxima of the native and various oxidized states of the MnP mutant proteins were essentially identical to those of the wild-type enzyme (Table 1), suggesting that substitution of amides for the acidic Mn^{II} binding ligands did not alter the heme environment of the protein significantly.

Table 1: Absorbance Maxima (nm) of Native and Oxidized Intermediates of Wild-Type MnP1 and MnP1 Mutants

enzyme	native	compound I	compound II
wt MnP1 ^a	406, 502, 632	407, 558, 617 sh, ^b 650	420, 528, 555
MnP D179N ^c	406, 502, 635	398, 557, 615 sh, 650	420, 528, 556
MnP E35Q	406, 502, 635	398, 558, 616 sh, 650	420, 528, 555
MnP E39Q	406, 501, 637	400, 557, 615 sh, 649	420, 528, 555
MnP E35Q-D179N	406, 500, 640	397, 555, 615 sh, 650	420, 528, 555

^a Wariishi et al. (1988). ^b Shoulder. ^c Kusters-van Someren et al. (1995).

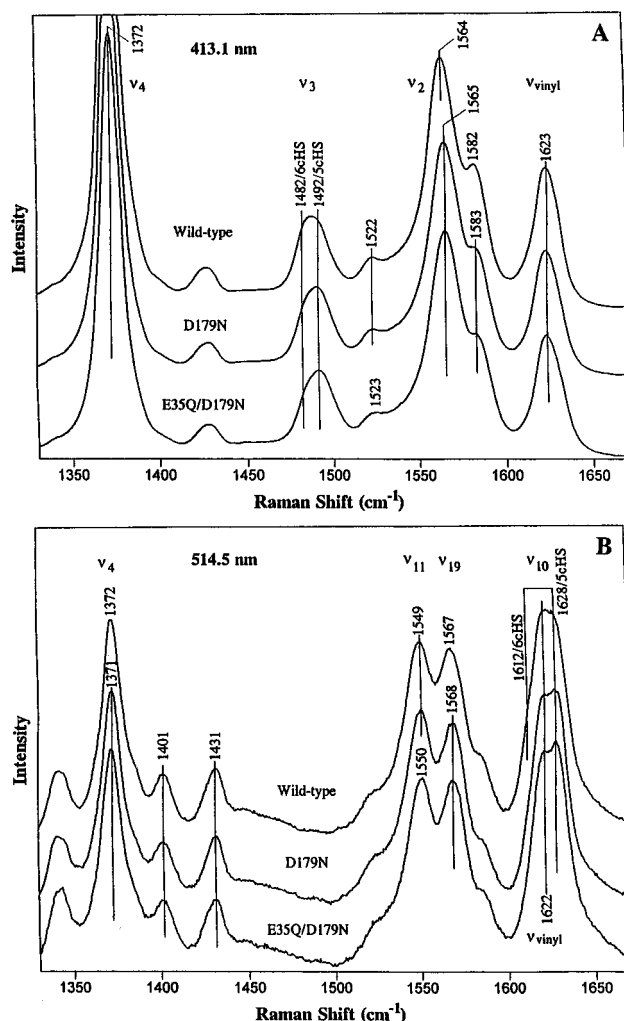


FIGURE 2: Resonance Raman spectra of MnP mutants. (A) Resonance Raman spectra of MnP proteins ($\sim 150 \mu\text{M}$ enzyme in 20 mM phosphate buffer, pH 6.0) obtained with Soret excitation (413.1 nm, 20 mW, 90° scattering geometry, ambient temperature). Samples are the wild-type enzyme (upper), and the mutant enzymes MnP D179N (middle) and E35Q-D179N (lower). Frequencies and assignments for selected heme bands are shown. (B) Resonance Raman spectra of MnP proteins ($\sim 150 \mu\text{M}$ enzyme in 20 mM phosphate buffer, pH 6.0) obtained with Q-band excitation (514.5 nm, 55 mW, 90° scattering geometry, ambient temperature). Samples are the same as in panel A. Frequencies and assignments for selected heme bands are shown. Polarization data were collected to support the assignments.

Resonance Raman Spectroscopy. The high-frequency (~ 1300 – 1700 cm^{-1}) rR spectral regions that are characteristic of heme coordination and spin state are shown in Figures 2A and 2B for Soret band (413.1-nm) and Q-band (514.5-nm) excitation, respectively. The rR spectrum of wild-type MnP (potassium phosphate buffer, pH 6.0, top

Table 2: Kinetic Parameters of Wild-Type MnP1, rMnP1, MnP D179N, MnP E35Q, MnP E39Q, and MnP E35Q-D179N^a

	K_m (μ M)		k_{cat} (s^{-1})/Mn ^{II}
	Mn ^{II}	H ₂ O ₂	
wt MnP1	73	42	3.0×10^2
rMnP1	69	39	2.9×10^2
MnP D179N	3.7×10^3	34	1.1
MnP E35Q	4.4×10^3	27	0.77
MnP E39Q	2.0×10^3	37	1.2
MnP E35Q-D179N	8.1×10^3	31	0.29

^a Reactions were carried out in 50 mM sodium malonate, pH 4.5. Apparent K_m and k_{cat} for Mn^{II} were determined using 0.1 mM H₂O₂. Apparent K_m for H₂O₂ was determined using 5.0 mM Mn^{II}.

trace) is of significantly higher quality and resolution than that reported previously (Mino et al., 1988). The new data show that the broad peak at 1487 cm⁻¹ (ν_3) is partially resolved into two components at 1482 and 1492 cm⁻¹ (Figure 2A) and that the peak at 1623 cm⁻¹ (C=C_{vinyl} and ν_{10}) consists of three components at ~1612, 1622, and 1628 cm⁻¹ (Figure 2B). Although the relative intensities of the 1482/1492 cm⁻¹ pair respond to changes in pH and ionic strength, both components are polarized (data not shown) and characteristic of ν_3 of six-coordinate high-spin (6cHS) and five-coordinate high-spin (5cHS) heme species, respectively. Consistent with the appearance of two ν_3 modes, the depolarized bands at ~1612 and 1628 cm⁻¹ (Figure 2B) are the corresponding ν_{10} porphyrin skeletal vibrations of 6cHS and 5cHS hemes, respectively. The band at 1622 cm⁻¹ in the 514.5-nm spectrum is polarized and therefore can be assigned to a C=C_{vinyl} stretching mode. This vinyl mode is almost totally responsible for the strongly polarized band at 1623 cm⁻¹ observed with Soret excitation (Figure 2A). The present data provide compelling evidence that native wild-type MnP contains a mixture of 6cHS and 5cHS heme species at room temperature.

The rR spectra of the D179N single (Kusters-van Someren et al., 1995) and the E35Q-D179N double mutations of acidic ligands in the Mn^{II} binding pocket were essentially identical to those of wild-type MnP (Figure 2A,B, lower traces). Hence, these mutations did not result in any significant perturbation to the heme moiety. Only minor changes in intensities, but no frequency shifts, were detectable in the heme vibrational spectra as a result of these mutations. For example, in the 413-nm spectra of both mutants (Figure 2A), the intensity of the 1492 cm⁻¹ component of ν_3 was increased relative to that at 1482 cm⁻¹, in contrast to the nearly equal intensities in the spectrum of the wild-type enzyme; in parallel, the proportion of the 1628/1612 cm⁻¹ ν_{10} components also was increased (Figure 2B), suggesting that a slightly greater proportion of the hemes in the mutants was in a 5cHS state.

Steady-State Kinetics. Under steady-state conditions, linear Lineweaver–Burk plots were obtained over a range of Mn^{II}, ferrocyanide, and H₂O₂ concentrations in 50 mM malonate, pH 4.5 (data not shown). The apparent K_m and k_{cat} values for Mn^{II}, ferrocyanide, and H₂O₂ are listed in Tables 2 and 3. The apparent K_m values for H₂O₂ (30–40 μ M) and ferrocyanide (3.3–3.6 mM) were similar for the wild-type MnP1, recombinant MnP1, and MnP mutant proteins. In contrast, the apparent K_m values for Mn^{II} of MnP E35Q and E39Q were ~60- and ~30-fold higher, respectively, than that for the wild-type MnP1 (Table 2),

Table 3: Kinetic Parameters of MnP Proteins for Ferrocyanide Oxidation^a

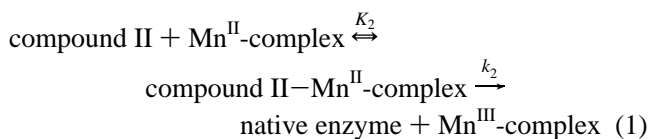
enzyme	K_m (mM)	k_{cat} (s^{-1})	k_{cat}/K_m ($M^{-1} s^{-1}$)
wt MnP1	3.6	5.3	1.5×10^3
rMnP1	3.5	5.6	1.6×10^3
MnP D179N	3.5	5.4	1.6×10^3
MnP E35Q	3.3	5.4	1.6×10^3
MnP E39Q	3.5	5.4	1.6×10^3
MnP E35Q-D179N	3.5	5.4	1.5×10^3

^a Reactions were carried out in 50 mM sodium malonate, pH 4.5. Apparent K_m and k_{cat} for ferrocyanide were determined using 0.1 mM H₂O₂.

whereas the apparent k_{cat} values of MnP E35Q and E39Q for Mn^{II} were 390- and 250-fold lower, respectively, than for the wild-type proteins. Furthermore, the apparent K_m value of the MnP E35Q-D179N double mutant for Mn^{II} was ~120-fold higher than that for wild-type MnP1. In addition, the apparent k_{cat} value of the MnP E35Q-D179N double mutant for Mn^{II} was approximately 1000 times lower than that for the wild-type MnP1 (Table 2).

Effect of Mutations on Compound I Formation. We demonstrated previously that the rate of MnP compound I formation was not affected by the structure or concentration of the organic acid chelator (Kishi et al., 1994). In our current work, the rate of MnP compound I formation was determined at pH 4.6 in 20 mM potassium succinate. Compound I formation was measured at 397 nm, an isosbestic point between compounds I and II, excluding interference from the possible reduction of compound I. The observed rate constants (k_{obs}) were linearly proportional to the H₂O₂ concentrations at 10–50-fold excess (data not shown). The second-order rate constants (k_{1app}) obtained for compound I formation for the wild-type protein and the mutant proteins D179N, E35Q, E39Q, and E35Q-D179N were similar (Table 4).

Effect of Mutations on Compound II Reduction. The rate of compound II reduction is the rate-limiting step in the MnP catalytic cycle (Wariishi et al., 1988, 1989a; Kishi et al., 1994; Kuan et al., 1993). The reductions of the wild-type and mutant proteins were followed at 406 nm under pseudo-first-order conditions using an excess of reducing substrate. The plots of observed pseudo-first-order rate constants versus Mn^{II} concentrations leveled off at high Mn^{II} concentration in 1 mM potassium oxalate (pH 4.6) (Figure 3). This reaction can be explained by a simple binding interaction between reactants, according to eqs 1–3:



$$k_{2obs} = k_2 / (1 + K_2 / [\text{Mn}^{\text{II}}\text{-complex}]) \quad (2)$$

$$K_2 = [\text{compound II}][\text{Mn}^{\text{II}}\text{-complex}] / [\text{compound II-Mn}^{\text{II}}\text{-complex}] \quad (3)$$

where k_2 is a first-order rate constant (s^{-1}) and K_2 is a dissociation constant (M). The calculated values for the first-order rate constant and the dissociation constant are listed in Table 5. The equilibrium dissociation constants for the MnP single and double mutants were approximately 100-

Table 4: Rate of Formation of MnP Compound I^a

MnP proteins	k_{1app} (M ⁻¹ s ⁻¹)
wt MnP1	$(1.3 \pm 0.1) \times 10^6$
MnP D179N	$(1.1 \pm 0.2) \times 10^6$
MnP E35Q	$(1.1 \pm 0.2) \times 10^6$
MnP E39Q	$(1.2 \pm 0.1) \times 10^6$
MnP E35Q-D179N	$(1.1 \pm 0.2) \times 10^6$

^a MnP compound I formation was followed at 397 nm, the isosbestic point between compounds I and II. Reactions were carried out in 20 mM potassium succinate, pH 4.6 (ionic strength 0.1 M). These rate constants were linearly proportional to [H₂O₂] with a zero intercept.

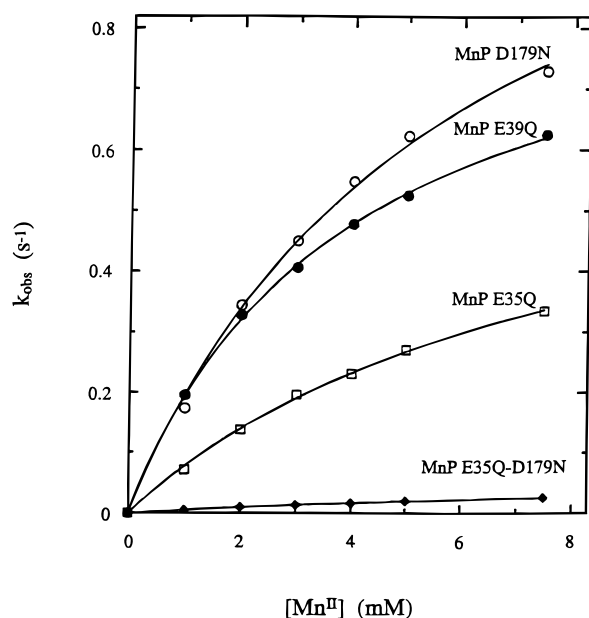


FIGURE 3: Kinetics of reduction of compound II of MnP mutant proteins by Mn^{II}. Reduction of compound II of MnP D179N (○), E39Q (●), E35Q (□), and E35Q-D179N (◆) by Mn^{II} in 1 mM potassium oxalate, pH 4.6. Each trace exhibited single-exponential character. Concentration of enzyme was 2 μM, ionic strength 0.1 M.

and 200-fold higher, respectively, than that for the wild-type protein. The first-order rate constants for the single mutants and the double mutant were approximately 200- and 4000-fold lower, respectively, than that for the wild-type protein.

The reduction of compound II to native enzyme also was measured with *p*-cresol and ferrocyanide as the substrates. The plots of pseudo-first-order rate constants versus *p*-cresol or ferrocyanide concentrations were linear for wild-type MnP1 and MnP mutant proteins (data not shown). The calculated second-order rate constants are listed in Table 6. The second-order rate constants of MnP mutants for *p*-cresol and ferrocyanide were similar to those of wild-type MnP1, demonstrating that these mutations did not affect the oxidation of these substrates.

DISCUSSION

Although the catalytic cycle of MnP is similar to that of other plant and fungal peroxidases (Gold et al., 1989; Gold & Alic, 1993; Wariishi et al., 1988, 1989a; Dunford & Stillman, 1976; Renganathan & Gold, 1986), this enzyme is unique in its ability to oxidize Mn^{II} to Mn^{III} (Glenn et al., 1986; Wariishi et al., 1989a,b, 1992). The latter, complexed with an organic acid such as oxalate, diffuses from the enzyme to oxidize either the terminal phenolic substrate

Table 5: Kinetic Parameters for Reduction of MnP Compound II by Mn^{II}^a

enzyme	first-order rate constants (s ⁻¹)	equilibrium dissociation constants (M)
wt MnP1 ^b	$(2.3 \pm 0.2) \times 10^2$	$(5.6 \pm 1.0) \times 10^{-5}$
MnP D179N ^c	1.3 ± 0.1	$(5.6 \pm 0.6) \times 10^{-3}$
MnP E35Q	0.69 ± 0.03	$(8.0 \pm 0.6) \times 10^{-3}$
MnP E39Q	0.94 ± 0.02	$(3.9 \pm 0.2) \times 10^{-3}$
MnP E35Q-D179N	$(6.0 \pm 0.3) \times 10^{-2}$	$(1.1 \pm 0.1) \times 10^{-2}$

^a Reactions were carried out in 1 mM potassium oxalate, pH 4.6, containing 2 μM MnP compound II. The ionic strength was adjusted to 0.1 M. ^b Kishi et al. (1994). ^c Kusters-van Someren et al. (1995).

Table 6: Kinetic Parameters for the Reduction of MnP Compound II by Ferrocyanide and *p*-Cresol^a

substrate	MnP proteins	second-order rate constant (M ⁻¹ s ⁻¹)
ferrocyanide	wt MnP1	$(1.2 \pm 0.1) \times 10^3$
	MnP D179N	$(1.1 \pm 0.2) \times 10^3$
	MnP E35Q	$(1.1 \pm 0.1) \times 10^3$
	MnP E39Q	nd ^b
	MnP E35Q-D179N	$(1.0 \pm 0.3) \times 10^3$
<i>p</i> -cresol	wt MnP1	$(1.9 \pm 0.2) \times 10^2$
	MnP D179N	$(1.6 \pm 0.3) \times 10^2$
	MnP E35Q	$(1.9 \pm 0.1) \times 10^2$
	MnP E39Q	$(1.4 \pm 0.4) \times 10^2$
	MnP E35Q-D179N	$(1.9 \pm 0.2) \times 10^2$

^a Reactions were conducted in 20 mM potassium malonate (pH 4.6, ionic strength 0.1 M), containing 2 μM MnP II. ^b Not determined.

(Glenn et al., 1986; Tuor et al., 1992) or a mediator (Bao et al., 1994; Wariishi et al., 1989b). The recent crystal structure (Sundaramoorthy et al., 1994), as well as homology modeling of MnP (Johnson et al., 1993), indicates that there is a cation binding site on the surface of the protein, consisting of the carboxylates of three acidic amino acid ligands, Asp179, Glu35, and Glu39, and one of the heme propionates. In the crystal structure (Sundaramoorthy et al., 1994), the final two ligands for the hexacoordinate Mn^{II} ion are water molecules, but these might be replaced by a chelator such as oxalate during the catalytic cycle. The characterization of our first site-directed MnP mutant, D179N, suggests that this cation site is the productive Mn^{II} binding site. Comparison of the Mn^{II} binding ligands in MnP and corresponding amino acid residues in the LiP-H8 crystal structure (Pribynow et al., 1989; Poulos et al., 1993; Piontek et al., 1993; Sundaramoorthy et al., 1994; Ritch & Gold, 1992) reveals that two of three anionic residues found in MnP are replaced by noncharged residues in LiP: Ala36 for Glu35 and Asn182 for Asp179. Only Glu39 in MnP is conserved as Glu40 in LiP. In addition, the heme propionate in LiP is not positioned for favorable Mn^{II} binding, and the location of the extended C-terminal peptide in LiP would interfere with Mn^{II} binding (Sundaramoorthy et al., 1994). Thus, LiP lacks an available, stable Mn^{II} binding site. Although it recently has been claimed that one of the LiP isozymes, H2, can oxidize Mn^{II} (Khindaria et al., 1995; Sutherland et al., 1995), comparison of the LiP-H2 sequence with those of MnP1 and LiP-H8 reveals that LiP-H2 also lacks a favorable Mn^{II} binding site, and thus is unlikely to complete its catalytic cycle in the presence of Mn^{II} as the only reducing substrate. Contamination of LiP-H2 with MnP during purification may account for the reported oxidation of Mn^{II} (Khindaria et al., 1995; Sutherland et al., 1995).

Mutation of each of the ligands in the Mn^{II} binding site of MnP would increase our understanding of the unique specificity of this peroxidase. Our earlier results indicate that the Asp179Asn mutation significantly affects the oxidation of Mn^{II}, probably by decreasing the affinity of the enzyme for Mn^{II}. However, these results did not rule out the possible involvement of Asp179 in electron transfer. To better understand how the Mn^{II} binding site ligands function, we have altered the other amino acid ligands in the Mn^{II} binding site: Glu35Gln, Glu39Gln, and Glu35Gln-Asp179Asn.

We recently demonstrated the homologous expression of recombinant MnP isozyme 1 (rMnP1) of *P. chrysosporium* (Mayfield et al., 1994b), wherein expression of the *mnp1* gene is under the control of the *P. chrysosporium* *gpd* gene promoter. This construct allows expression of rMnP1 during the primary metabolic phase of growth when endogenous MnP is not expressed. Both the spectral and kinetic properties of the recombinant enzyme are very similar to wild-type MnP1, indicating that this expression system is suitable for conducting structure/function studies of MnP by site-directed mutagenesis. Overlap extension PCR was used to create the E35Q, E39Q, and E35Q-D179N mutations. The mutant gene, in pOGI18, was transformed into the Adel strain of *P. chrysosporium* as described (Kusters-van Someren et al., 1995). Each mutant protein was purified to homogeneity by a combination of hydrophobic interaction, Blue agarose, and anion-exchange chromatographies.

As with the MnP D179N mutant (Kusters-van Someren et al., 1995), the MnP E35Q, E39Q, and E35Q-D179N mutant proteins are essentially identical to the wild-type enzyme with respect to chromatographic properties and molecular weight, suggesting that these mutations do not lead to gross conformational alterations of the protein. Furthermore, the E35Q, E39Q, and E35Q-D179N mutant, native ferric proteins exhibit essentially identical spectral features to that of wild-type MnP1 (Figure 1, Table 1) (Wariishi et al., 1988; Mayfield et al., 1994b). The spectra of the catalytic intermediates, compounds I and II, of the mutant proteins also are essentially identical to those of the wild-type MnP oxidized intermediates (Figure 1, Table 1), suggesting that the heme environment of MnP is not altered significantly by E35Q, E39Q, and E35Q-D179N mutations in the Mn^{II} binding site.

Resonance Raman spectroscopy is particularly well suited for the determination of coordination and spin states of hemes and metalloporphyrins (Spiro, 1988). Of the many porphyrin skeletal vibrational modes, ν_3 and ν_{10} are generally easily identified and, hence, serve as very useful indicators. Characteristic ν_3 values are ~ 1480 , ~ 1490 , and ~ 1505 cm⁻¹ for 6cHS, 5cHS, and 6cLS hemes, respectively. The corresponding set of ν_{10} values are ~ 1610 , ~ 1625 , and ~ 1640 cm⁻¹ (Mino et al., 1988; Sun et al., 1993, 1994).

The rR results for wild-type MnP have been obtained at higher resolution and superior S/N as compared to an earlier report from this laboratory (Mino et al., 1988) and show the coexistence of 6cHS and 5cHS heme species at room temperature. The mixture of species is consistent with the presence of a six-coordinate, water-bound heme in equilibrium with a five-coordinate heme lacking an aqua ligand in the distal heme pocket. In the crystal structure of native wild-type MnP, a water molecule is located between the Fe^{III} atom of the heme and the distal His46, with an Fe—OH₂ distance of 2.88 Å (Sundaramoorthy et al., 1994). Similar

coordination-state equilibria have been proposed for LiP and cytochrome *c* peroxidase in acidic to neutral buffers (Andersson et al., 1987; Smulevich et al., 1988). The Fe—OH₂ distances in the crystal structures of LiP and cytochrome *c* peroxidase are between 2.42 and 2.73 Å (Poulos et al., 1993; Finzel et al., 1984).

Furthermore, mutations D179N and E35Q-D179N appear to have little or no effect on the structure and coordination-state equilibrium of the heme. Although these residues are involved in the formation of a Mn^{II} ion binding site near the heme, one of whose propionate side chains also is implicated as a ligand to the cation site, our UV/vis and resonance Raman data suggest that perturbations caused by removal of these acidic residue(s) from the cation binding site are not transmitted to the nearby heme in a manner detectable by these spectroscopic methods.

In contrast to the negligible effects of these mutations on the spectroscopic properties of MnP, mutations of the Mn^{II} binding ligands change the catalytic properties of MnP dramatically. The turnover numbers (k_{cat}) for Mn^{II} oxidation by MnP E35Q and E39Q decrease 300-fold with respect to the wild-type enzyme. The apparent K_m values for MnP E35Q and E39Q are 60 and 30 times higher, respectively, than that for wild-type MnP (Table 2). Furthermore, the k_{cat} for Mn^{II} oxidation by the E35Q-D179N double mutant decreases 1000-fold, and the K_m for this double mutant increases 110-fold with respect to the wild-type enzyme (Table 2).

These mutations also have a dramatic effect on the reduction of compound II to the native enzyme by Mn^{II} (Figure 3), which is the rate-limiting step in the MnP catalytic cycle (Wariishi et al., 1988, 1989a; Kishi et al., 1994; Kuan et al., 1993). At 1 mM oxalate (pH 4.6), the plots of k_{obs} versus Mn^{II} concentration are hyperbolic (Figure 3), indicating a binding interaction between Mn^{II} and MnP. The equilibrium dissociation constants for compound II reduction for the MnP single mutants increase ~ 100 -fold and for the double mutant, ~ 200 -fold (Table 5), indicating that the binding affinity of the mutant proteins for Mn^{II} is significantly decreased with respect to the wild-type protein. The first-order rate constants for the MnP E35Q, E39Q, and E35Q-D179N proteins are approximately 300-, 200-, and 4000-fold lower, respectively, than the value obtained for wild-type MnP (Table 5), strongly suggesting that this Mn^{II} binding site is the productive, and probably the only, substrate oxidation site. The effect of the mutations on the first-order rate constant suggests that the electron-transfer rate is lowered (eqs 1–3). This may be a consequence of a higher redox potential for Mn^{II} in the Mn binding site of the mutant proteins as compared with that for the wild-type protein. Alternatively, it may represent a much slower rate of electron transfer from a second, weaker Mn binding site.

Interestingly, the K_m and k_{cat} values indicate that oxidation of ferrocyanide by MnP (Table 3) is not affected by these mutations in the Mn^{II} binding site of MnP. Furthermore, the similarity of the second-order rate constants for MnP compound II reduction by *p*-cresol and ferrocyanide for the mutant and wild-type proteins (Table 6) indicates that these reactions are not affected by mutations in the Mn^{II} binding site. These results indicate that neither ferrocyanide nor *p*-cresol binds or is oxidized at the Mn^{II} binding site.

Furthermore, the mutations do not affect either the apparent K_m for H₂O₂ (Table 2) or the pre-steady-state rate

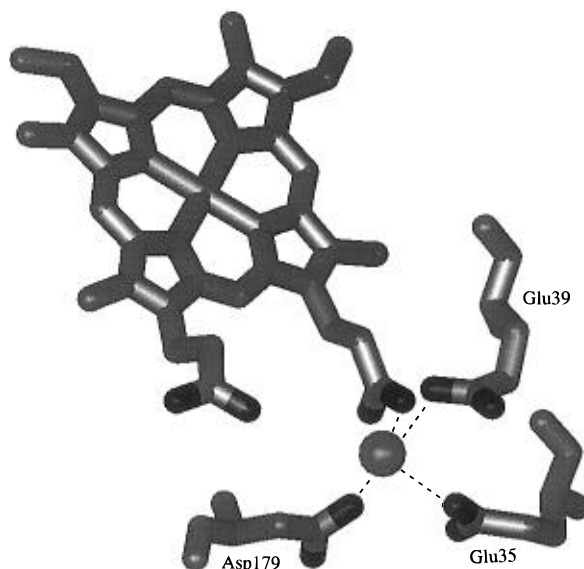


FIGURE 4: Mn^{II} binding site of MnP showing four acid ligands: D179, E35, E39, and a heme propionate (Sundaramoorthy et al., 1994).

of compound I formation by H_2O_2 (Table 4). This suggests that the environment of the amino acid residues involved in the formation of compound I, including the distal His, distal Arg, and proximal His, has not been altered by any of the mutations in the Mn^{II} binding site. The recent crystal structure of MnP clearly shows that the peroxide and aromatic access channel is distinct from the Mn^{II} binding site on the surface of the protein.

Homology modeling (Johnson et al., 1993) and the MnP crystal structure (Sundaramoorthy et al., 1994) predict that the Mn^{II} binding site in MnP consists of the acidic amino acids Asp179, Glu35, and Glu39, and a heme propionate. However, homology modeling also predicts several alternate Mn^{II} binding sites (Johnson et al., 1993). Although it is possible that there are other Mn^{II} binding sites, the results presented here strongly suggest the Mn^{II} binding site shown in Figure 4 (Sundaramoorthy et al., 1994) is the only productive catalytic site for Mn^{II} oxidation, particularly since the double mutation, E35Q-D179N, almost completely destroys MnP oxidation of Mn^{II} (Tables 2 and 5).

In conclusion, the results presented in this study, along with our previous work (Kusters-van Someren et al., 1995), demonstrate that changing any of the acidic amino acid Mn^{II} ligands, Asp179, Glu35, or Glu39, significantly affects the oxidation of Mn^{II} , most probably by decreasing the affinity of the enzyme for Mn^{II} . In contrast, neither the rate of formation of compound I nor the rate of reduction of compound II by *p*-cresol or ferrocyanide is affected by these mutations. These results indicate that the Mn^{II} binding site consisting of Asp179, Glu35, and Glu39 is the productive site. The coordination of Mn^{II} at this site is octahedral, which is typical of Mn^{II} coordination complexes (Demmer et al., 1980). Current views envision electron transfer pathways through covalent bonds in proteins (Onuchic & Bertram, 1990). The structure of this site suggests that the electron may be transferred from Mn^{II} to the porphyrin via the heme propionate ligand, using a nearly continuous σ -bonded path. Additional mechanistic, structural, and mutagenesis studies will be required to elucidate further the electron transfer pathway in this system.

REFERENCES

- Alic, M., Letzring, C., & Gold, M. H. (1987) *Appl. Environ. Microbiol.* 53, 1464–1469.
- Alic, M., Clark, E. K., Kornegay, J. R., & Gold, M. H. (1990) *Curr. Genet.* 17, 305–311.
- Andersson, L. A., Renganathan, V., Loehr, T. M., & Gold, M. H. (1987) *Biochemistry* 26, 2258–2263.
- Banci, L., Bertini, I., Pease, E. A., Tien, M., & Turano, P. (1992) *Biochemistry* 31, 10009–10017.
- Bao, W., Fukushima, Y., Jensen, K. A., Moen, M. A., & Hammel, K. E. (1994) *FEBS Lett.* 354, 297–300.
- Bumpus, J. A., & Aust, S. D. (1987) *BioEssays* 6, 166–170.
- Buswell, J. A., & Odier, E. (1987) *CRC Crit. Rev. Biotechnol.* 6, 1–60.
- Cheddar, G., Meyer, T. E., Cusanovich, M. A., Stout, C. D., & Tollin, G. (1989) *Biochemistry* 28, 6318–6322.
- Cotton, M. L., & Dunford, H. B. (1973) *Can. J. Chem.* 51, 582–587.
- Demmer, H., Hinz, I., Keller-Rudex, H., Koeber, K., Kottelwesch, H., & Schneider, D. (1980) in *Coordination Compounds of Manganese* (Schleitzer-Rust, E., Ed.) 8th ed., Vol. 56, pp 1–185, Springer-Verlag, New York.
- Dunford, H. B., & Stillman, J. S. (1976) *Coord. Chem. Rev.* 19, 187–251.
- Edwards, S. L., Raag, R., Wariishi, H., Gold, M. H., & Poulos, T. L. (1993) *Proc. Natl. Acad. Sci. U.S.A.* 90, 750–754.
- Finzel, B. C., Poulos, T. L., & Kraut, J. (1984) *J. Biol. Chem.* 259, 13027–13036.
- Glenn, J. K., & Gold, M. H. (1985) *Arch. Biochem. Biophys.* 242, 329–341.
- Glenn, J. K., Akileswaran, L., & Gold, M. H. (1986) *Arch. Biochem. Biophys.* 251, 688–696.
- Godfrey, B. J., Mayfield, M. B., Brown, J. A., & Gold, M. H. (1990) *Gene* 93, 119–124.
- Godfrey, B. J., Akileswaran, L., & Gold, M. H. (1994) *Appl. Environ. Microbiol.* 60, 1353–1358.
- Gold, M. H., & Alic, M. (1993) *Microbiol. Rev.* 57, 605–622.
- Gold, M. H., Cheng, T. M., & Mayfield, M. B. (1982) *Appl. Environ. Microbiol.* 44, 996–1000.
- Gold, M. H., Wariishi, H., & Valli, K. (1989) *ACS Symp. Ser.* 389, 127–140.
- Hammel, K. E. (1989) *Enzyme Microb. Technol.* 11, 776–777.
- Hammel, K. E., Jensen, K. A., Jr., Mozuch, M. D., Landucci, L. L., Tien, M., & Pease, E. A. (1993) *J. Biol. Chem.* 268, 12274–12281.
- Harris, R. Z., Wariishi, H., Gold, M. H., & Ortiz de Montellano, P. R. (1991) *J. Biol. Chem.* 266, 8751–8758.
- Hatakka, A. (1994) *FEMS Microbiol. Rev.* 13, 125–135.
- Ho, S. N., Hunt, H. D., Horton, R. M., Pullen, J. K., & Pease, L. R. (1989) *Gene* 77, 51–59.
- Johnson, F., Loew, G. H., & Du, P. (1993) in *Plant Peroxidases: Biochemistry and Physiology* (Welinder, K. G., Rasmussen, S. K., Penel, C., & Greppin, H., Eds.) pp 31–34, University of Geneva, Geneva, Switzerland.
- Joshi, D., & Gold, M. H. (1993) *Appl. Environ. Microbiol.* 59, 1779–1785.
- Khindaria, A., Barr, D. P., & Aust, S. D. (1995) *Biochemistry* 34, 7773–7779.
- Kirk, T. K., & Farrell, R. L. (1987) *Annu. Rev. Microbiol.* 41, 465–505.
- Kishi, K., Wariishi, H., Marquez, L., Dunford, H. B., & Gold, M. H. (1994) *Biochemistry* 33, 8694–8701.
- Kuan, I.-C., Johnson, K. A., & Tien, M. (1993) *J. Biol. Chem.* 268, 20064–20070.
- Kusters-van Someren, M., Kishi, K., Lundell, T., & Gold, M. H. (1995) *Biochemistry* 34, 10620–10627.
- Laemmli, U. K. (1970) *Nature* 227, 680–685.
- Mayfield, M. B., Godfrey, B. J., & Gold, M. H. (1994a) *Gene* 142, 231–235.
- Mayfield, M. B., Kishi, K., Alic, M., & Gold, M. H. (1994b) *Appl. Environ. Microbiol.* 60, 4303–4309.
- Mino, Y., Wariishi, H., Blackburn, N. J., Loehr, T. M., & Gold, M. H. (1988) *J. Biol. Chem.* 263, 7029–7036.
- Onuchic, J. N., & Bertram, D. N. (1990) *J. Chem. Phys.* 92, 722–733.

- Orth, A. B., Royce, D. J., & Tien, M. (1993) *Appl. Environ. Microbiol.* 59, 4017–4023.
- Pease, E. A., Andrawis, A., & Tien, M. (1989) *J. Biol. Chem.* 264, 13531–13535.
- Perie, F. H., & Gold, M. H. (1991) *Appl. Environ. Microbiol.* 57, 2240–2245.
- Piontek, K., Glumoff, T., & Winterhalter, K. (1993) *FEBS Lett.* 315, 119–124.
- Poulos, T. L., Edwards, S., Wariishi, H., & Gold, M. H. (1993) *J. Biol. Chem.* 268, 4429–4440.
- Pribnow, D., Mayfield, M. B., Nipper, V. J., Brown, J. A., & Gold, M. H. (1989) *J. Biol. Chem.* 264, 5036–5040.
- Renganathan, V., & Gold, M. H. (1986) *Biochemistry* 25, 1626–1631.
- Ritch, T. G., Jr., & Gold, M. H. (1992) *Gene* 118, 73–80.
- Sambrook, S. J., Fritsch, E. F., & Maniatis, T. (1989) *Molecular Cloning: A Laboratory Manual*, Cold Spring Harbor Laboratory Press, Cold Spring Harbor, NY.
- Smulevich, G., Mauro, J. M., Fishel, L. A., English, A. M., Kraut, J., & Spiro, T. G. (1988) *Biochemistry* 27, 5477–5485.
- Spiro, T. G., Ed. (1988) *Biological Applications of Raman Spectroscopy, Vol. III, Resonance Raman Spectra of Hemes and Metalloproteins*, Wiley, New York.
- Sun, J., Wilks, A., Ortiz de Montellano, P. R., & Loehr, T. M. (1993) *Biochemistry* 32, 14151–14157.
- Sun, J., Loehr, T. M., Wilks, A., & Ortiz de Montellano, P. R. (1994) *Biochemistry* 33, 13734–13740.
- Sundaramoorthy, M., Kishi, K., Gold, M. H., & Poulos, T. L. (1994) *J. Biol. Chem.* 269, 32759–32767.
- Sutherland, G. R. J., Khindaria, A., Chung, N., & Aust, S. D. (1995) *Biochemistry* 34, 12624–12629.
- Tuor, U., Wariishi, H., Schoemaker, H. E., & Gold, M. H. (1992) *Biochemistry* 31, 4986–4995.
- Valli, K., & Gold, M. H. (1991) *J. Bacteriol.* 173, 345–352.
- Valli, K., Wariishi, H., & Gold, M. H. (1992) *J. Bacteriol.* 174, 2131–2137.
- Wariishi, H., Akileswaran, L., & Gold, M. H. (1988) *Biochemistry* 27, 5365–5370.
- Wariishi, H., Dunford, H. B., MacDonald, I. D., & Gold, M. H. (1989a) *J. Biol. Chem.* 264, 3335–3340.
- Wariishi, H., Valli, K., Renganathan, V., & Gold, M. H. (1989b) *J. Biol. Chem.* 264, 14185–14191.
- Wariishi, H., Valli, K., & Gold, M. H. (1991) *Biochem. Biophys. Res. Commun.* 176, 269–275.
- Wariishi, H., Valli, K., & Gold, M. H. (1992) *J. Biol. Chem.* 267, 23688–23695.

BI960679C